



JAAS

**High Resolution Plutonium-239/240 Mixture Alpha Spectroscopy using Centrifugally Tensioned Metastable Fluid Detector Sensor Technology**

Journal:	<i>Journal of Analytical Atomic Spectrometry</i>
Manuscript ID	JA-ART-08-2021-000285.R2
Article Type:	Paper
Date Submitted by the Author:	05-Nov-2021
Complete List of Authors:	Harabagiu, Catalin; Purdue University Boyle, Nathan; Purdue University Archambault, Brian; Pacific Northwest National Laboratory DiPrete, David; Savannah River National Laboratory Taleyarkhan, Rusi; Purdue University,

SCHOLARONE™  
Manuscripts

# High Resolution Plutonium-239/240 Mixture Alpha Spectroscopy using Centrifugally Tensioned Metastable Fluid Detector Sensor Technology

By:

Catalin Harabagiu<sup>1</sup>, Nathan Boyle<sup>1,2\*\*</sup>, Brian Archambault<sup>1,3\*\*</sup>,

David DiPrete<sup>1,4</sup>, Rusi Taleyarkhan<sup>1\*</sup>

1 – Purdue University, West Lafayette, IN, USA; 2 – U.S. Intelligence Community Post-Doctoral Fellow, ORISE, Oak Ridge, TN, USA;

3 – Pacific Northwest National Laboratory, Richland, WA, USA; 4 – Savannah River National Laboratory, Aiken, SC, USA

(\*) – Corresponding Author (Email: [rusi@purdue.edu](mailto:rusi@purdue.edu)); (\*\*) – research content developed while at Purdue University.

## Abstract

This paper presents a novel and rapid, wet chemistry technique for spectroscopically detecting trace ( $\sim 10^{-3}$  Bq/mL) level alpha emitting radionuclides mixtures with under 10 keV alpha energy resolution. The Centrifugally Tensioned Metastable Fluid Detector (CTMFD) sensor technology with a  $\sim 16$  mL sensitive volume was utilized and adapted for the ability to decipher trace level Pu-239 and Pu-240 content in mixtures of these two isotopes ranging in content from 1:0 to 0:1 in relative proportions with gamma-beta rejection, and  $\sim 100\%$  ( $4\pi$ ) alpha detection sensitivity validated for accuracy (within  $\pm 5\%$ ) against NIST standards. Pu-239 and Pu-240 isotopes emit closely spaced ( $< 10$  keV separated) energetic alpha particles and constitute a known challenge to decipher without resort to microcalorimetry or mass spectrometry. For the work presented in this paper, a relatively rapid ( $< 1$ h) sampling protocol was developed to create mixtures of these isotopes for CTMFD based examination and to derive the mixture's characteristic response function, viz., alpha decay detection rate over a range of tensioned metastable state negative pressure spanning the detection thresholds for the two isotopes. An accompanying methodology and algorithm were developed to analyze-deconvolute the Pu isotopes bearing mixture's response curves, and to determine the composition of each isotope within the mixture. Results based on experiments revealed this technique identified the Pu-239:Pu-240 isotopic activity ratio combinations within  $\pm 12\%$  for each of the samples ranging from 1:0, 5:1, 1:1, to 0:1 ratios – enabling alpha spectroscopy within few hours of counting, for an arbitrary Pu-239:Pu-240 ( $\sim 10^{-3}$  Bq/mL) mixture, using a single  $\sim 16$  mL CTMFD apparatus.

Keywords: CTMFD, High Resolution, Alpha-Spectroscopy, Pu-239/240, Actinide, Mixture

## Symbols/Acronyms:

CDE	= Cavitation detection event
CTMFD	=Centrifugally tensioned metastable fluid detector
DFP	= Decafluoropentane ( $C_5H_4F_{10}$ )
E	= Energy
$f$	= Rotation frequency
$r$	= Radius ( $r_m$ – meniscus separation distance; $r_b$ = distance of sensitive zone from centerline)
LET	= Linear energy transfer
LSS	= Liquid scintillation spectrometry
MS	= Mass spectrometry
NIST	= National Institute of Standards and Technology (USA)
PIPS	= Passive implanted planar silicon
$P_{neg}$	= Negative (Tensioned state) pressure
SV	= Sensitive volume
$V_b$	= Volume of central detection bulb of CTMFD correspond to radius $r = r_b$ (Eq. 4)
$\alpha$	= Alpha radiation particle
$\rho$	= Fluid density

## 1. Introduction

Alpha radiation monitoring is of significant importance in a multitude of arenas spanning nuclear medicine, radiation health physics, to nuclear energy, for combating nuclear terrorism and environmental sampling. A well-known challenge involves determination of the relative ratios of alpha emitting Pu-239 and Pu-240 isotopes in an unknown Pu isotopes-bearing sample – which can then provide critical non-proliferation and treaty verification pertaining forensic evidence (i.e., reactor versus weapons-grade production) [1]. The source of a Pu based special nuclear material (SNM) may be deduced from its Pu-239:Pu-240 ratio, which varies from ~10:1 (for weapons grade) to ~2:1 (for reactor grade); it should be noted that reactor grade Pu also include Pu-238 alpha emissions which are well separated in energy from Pu-239/240 emissions and easily detected by CTMFDs as discussed subsequently). While numerous isotopes spontaneously decay to emit readily detectable gamma-beta radiation, only a relatively few (mainly actinides) emit alpha particles which are much more difficult to detect and characterize, mainly because of their relatively 1000x higher stopping power. Besides deciphering for alpha radiation itself, an even greater challenge presents itself for spectroscopic identification of alpha particles emitted in a combination of alpha decaying isotopes, even of the same element and/or isotope.

General alpha particle detection can be performed using semiconductor, scintillation, proportional counters as also with nuclear track detectors [2]. For spectroscopically resolving alpha particle energies with ~30-100+ keV type resolution, the passive implanted planar silicon (PIPS) spectroscopic semiconductor detection technology and liquid scintillation spectrometers (LSS) are commonly used approaches. However, in order to decipher alpha emission energies with  $\leq 10$  keV type resolution, mass spectroscopy (IC-MS/ ICP-MS) [3-5], or microcalorimetry-cryogenic techniques [6] are used to detect and quantify coelutions of isotopic components. Several of such detection systems must also contend with natural background radiation effects (esp. from photon radiation), as also to consider environmental conditions of temperature, moisture (esp. condensing), shock, electromagnetic, dust and omnipresent electronic noise.

The goal of this paper is to present a novel approach and accompanying evidence for high resolution (< 10 keV) alpha spectroscopy and isotopic ratio identification based on the science and technology underlying the TMFD sensor technology [7-12] which is based on radiation interacting with atoms in fluids that are selectively placed under tensioned metastable states. One must recognize that all scientific techniques have their pros and cons. In order that practitioners can draw their own conclusions related to appropriateness of the TMFD based technique in comparison to other existing techniques, this paper includes details concerning detection sensitivity-efficiency, impact of background radiation, along with protocols to be followed and associated times for sample preparation, counting for alpha emission events, and use of the as-developed methodology for data unfolding to arrive at isotopic ratios, and associated alpha energy spectra. A brief background on the underlying science and operational principles is presented first, followed with description on how TMFDs were adapted for providing high-resolution, trace-level alpha spectroscopy.

### 1.1 Background on TMFDs and Modeling Framework for Mixed Isotope Alpha Spectrometry

Not well known is that fluids, like solids, can be tensioned and placed under negative (sub-vacuum) pressures. When tensioned, the fluid becomes metastable and the bonds holding the molecules together can be weakened sufficiently so that external stimuli can break these bonds and create audible-visible-recordable cavitation detection events (CDEs) in the form of vapor bubbles that quickly (within microseconds) grow from a few nanometers to several millimeters in diameter. TMFDs exploit this behavior of fluids at negative pressures to monitor for high linear energy transfer (LET) ionizing radiation

such as neutrons, alphas, and fission fragments to enable spectroscopic detection while remaining 100% blind to low LET ionizing radiation (e.g., gammas and betas) even under  $\sim 10^4$  R/h conditions [10]. This section will provide a brief introduction into the fundamental principles governing tensioned metastable fluid detectors.

TMFDs operate by tensioning the detector fluid, stretching the bonds holding the molecules together and placing the fluid in a state of metastability at subvacuum pressures. The tensioning of the fluid constantly pulls at the molecules, analogous to a rubber band being tensioned from both ends. The weakened molecular bonds can be broken when a nuclear particle interacts with the fluid, depositing enough energy to tear the fluid apart and induce a cavitation detection event (CDE) similar to how a tensioned rubber band snaps if a large enough puncture is made. TMFDs induce tensioned negative pressure states via one of two methods: acoustically or centrifugally. The research presented in this paper utilized the Centrifugally Tensioned Metastable Fluid Detector (CTMFD) sensor technology.

### *Figure 1*

The CTMFD induces  $P_{neg}$  states by rotating the diamond-shaped container bearing the sensing fluid about its central axis, as shown in Fig. 1. The  $P_{neg}$  values can be estimated in general form using the well-known Bernoulli law for incompressible fluids (and neglecting body forces) using Eqn. (1a) for any arbitrary radius ( $r$ ) as:

$$P_{neg}(r) = 2 * \pi^2 * \rho * f^2 * (r_m^2 - r^2) - P_{amb} \quad (1)$$

and, for representing the threshold tension state for sensitivity till the radial distance ( $r_b$ ) as,

$$P_{neg,thresh} = 2 * \pi^2 * \rho * f^2 * (r_m^2 - r_b^2) - P_{amb} \quad (2)$$

where,  $P_{neg,thresh}$  is the “negative pressure” state at a radius  $r_b$  from the centerline in the central bulb below which the liquid is sensitive,  $\rho$  is the density of the sensor fluid,  $f$  is the rotational frequency,  $r_m$  is the average radial separation above the arms, and  $P_{amb}$  is the ambient pressure. *Note, that the negative pressure states quoted in this paper, e.g.,  $P_{neg} = 0.1$  MPa or 1 bar, actually means that the fluid pressure is negative or sub-vacuum, i.e.,  $-0.1$  MPa ( $-1$  bar).* Upon reaching an appropriately high  $P_{neg}$  state, the interaction with a particle of a high enough energy and linear energy transfer (LET) such as fast neutrons, fission fragments and alpha emission can lead to CDEs which manifest themselves as fast (within microseconds) growing bubbles that are audible, visible and electronically timed-recorded (e.g., via light-beam interrupt signals or acoustic waves), as illustrated in Fig. 2 (without the need for light-tight photomultiplier tubes, charge collection trains, pulse-shape discrimination, high voltage sources and associated electronic noise, vacuum chambers or quenching related challenges).

*Figure 2***1.2 Relation to Past Studies, Enablements & Challenges on High Resolution Alpha Detection with CTMFDs**

Our past studies for CTMFD based detection of alpha emitters [7] such as Pu-238, Am-241, etc. were conducted for single individual isotopes and we had shown that 100% gamma blind, high ( $4\pi$ ) intrinsic efficiency (>95%) alpha decay detection is possible with CTMFDs which have been directly validated [8,9] using certified standards supplied by the United States National Institute of Standards and Technology (NIST). These attributes permitted detection at trace concentration levels – with 10-100x higher sensitivity than with our Beckman LS6500™ liquid scintillation spectrometer. For individual isotopes such as Pu-238 and Pu-239 with peak-to-peak separations of ~350 keV we could readily decipher for the ratios of these isotopes in mixtures. Notably, we could *individually* obtain separated (yet closely spaced) response curves for Pu-238 and Am-241 alpha emitters for which the recoil nuclei energies are only ~1.4 keV apart. The dominant alpha emission energies for Pu-238 and Am-241 are ~ 5.59 MeV and ~5.486 MeV, respectively (~ 10 keV separation between the dominant alpha energies and ~3 keV separation in the energy of the recoil nuclei). This situation is similar to the difference between the dominant alpha energy emission levels for Pu-239 and Pu-240 –the current challenge is to be able to decipher for the ratio when these isotopes are in mixture form. For the present work, we focus on the challenge of deciphering each of the two close alpha energy emitting isotopes Pu-239 and Pu-240 when in mixtures.

Furthermore, each isotope of Pu-239 and Pu-240 both possess a dominant and secondary branch in various proportions (along with the associated  $P_{neg}$  thresholds – not including speed control error) as shown in Table 1 and also must be considered for relative impact on spectroscopic identification of emissions from Pu-239 vs Pu-240.

**Table 1. Alpha & Recoil Nucleus Emission Energies for Pu-239 and Pu-240**

<b>Pu Isotope</b>	<b>Branching Ratio [%]</b>	<b>E Alpha [MeV]</b>	<b>E Recoil Nucleus [keV]</b>	<b><math>P_{neg}</math> Threshold (est.) (bar)</b>
239	70.8	5.156	87.772	4.15
239	17.1	5.144	87.562	4.25
239	11.9	5.105	86.902	4.3
240	72.8	5.168	87.596	4.35
240	27.2	5.123	86.842	4.4

Table 1 indicates that the alpha energies and the associated daughter recoil energies of Pu-239 and Pu-240 are almost identical, illustrating the difficulty for traditional alpha detectors (including PIPS based) to resolve these energies. Notable is the fact that despite the fact that the dominant  $E_\alpha$  (=5.156MeV) for Pu-239 is lower than the corresponding  $E_\alpha$  (=5.168 MeV) for Pu-240, the recoil nucleus energy levels are reversed in magnitude and separated by ~ 0.2 keV – i.e., 87.772 keV for Pu-239 less 87.596 keV for Pu-240. Nucleation of bubbles leading to cavitation detection events (CDEs) in TMFDs are largely caused by higher LET ions (which deposit their energy over shorter ranges) even though the alpha particle will also contribute some of its energy while traversing past the critical radius for nucleation; therefore, paradoxically, the corresponding  $P_{neg,thresh}$  for Pu-239 can be expected to be lower than that for Pu-240. One also must account for the contribution to detection rates from the associated (lower) energy alpha particle emissions from the same isotope. In order to account for such nuances, and to be able to identify for the

content of such alpha emitting isotopes without need to resort to mass-spectrometry, a novel method for ascertaining isotopic ratios was developed and will now be discussed.

## 2. Modeling Framework

This section discusses the theoretical framework for enabling one to resolve for relative ratios of the two closely-spaced (<10 keV) alpha emitting isotopes in a given mixture of Pu-239 and Pu-240.

### 2.1 Development of Response Curves

Equation 1 described how to evaluate for the negative pressure state at any point  $r_b$  in the radial direction from the centerline of the bulb region. Consequently, for a given value of  $r_b$  and  $r_m$ , the  $P_{neg}$  state is only a function of the rotational frequency, which can readily be tailored, providing the CTMFD with selective sensitivity and energy discrimination capabilities. Notably, for alpha spectroscopy, the CTMFD remains completely insensitive to the radiation energy imparted to the atoms in the sensing fluid until the threshold negative pressure state “ $P_{neg,thresh}$ ” is first reached (which first occurs for  $r_b = 0$ ) at the centerline in the bulb and then progresses outwards. This negative pressure state is determined to be the onset of sensitivity for detecting the alpha decay event for that isotope. As the frequency of rotation increases, the radius ( $r_b$ ) at which the fluid reaches the required  $P_{neg,thresh}$  state for detecting the specific alpha decay events also expands, as more and more of the central bulb becomes sensitive as evidenced from Eq. 2. For this work, a  $P_{neg}$  sweep was performed to determine the average count rate at each negative pressure state from onset of sensitivity to full sensitivity for each isotope of plutonium.

Figure 3 shows an example of a  $P_{neg}$  sweep as measured in a ~15-16 mL (central bulb ) sensitive volume (SV) CTMFD containing Pu-240 dissolved in the sensor fluid at a concentration of ~0.001 Bq/cc giving rise to a count rate of ~1.3 cpm when the entire SV has reached the required  $P_{neg}$  (~4.3 bar @ onset) threshold for detecting alpha emissions from Pu-240 decay. For the balance of this paper,  $P_{neg}/P_{thresh}$  values are quoted in “bar” units (1 bar = 0.1 MPa). Note also, that unless otherwise mentioned, the quoted values of  $P_{neg}$  represent the fluid tensioned pressure state along the centerline (i.e.,  $r=0$ ).

#### *Figure 3.*

From Figure 3, it is seen that as  $P_{neg}$  ( $r_b=0$ ) increases starting with sensitivity to the primary  $E_\alpha$ , the count rate increases as the detection volume increases (including with the contribution to detection from the secondary alpha emissions) until a full bulb sensitivity is reached when  $P_{neg}$  (@  $r_b \sim 25\text{mm}$ ) reaches  $P_{neg,thresh}$ . At this stage, when  $P_{neg}$  (@  $r_b = 0$ ) is ~4.8bar, the CDEs from primary and secondary alpha emissions are all contributive. One can estimate for the required rotational frequency to reach the experimentally derived value for  $P_{neg,thresh}$  for any given alpha emitting nuclide by setting  $r_b=0$  in Eq.(2) to obtain the corresponding  $P_{neg}$  state in the centerline (CL):

$$P_{neg,CL} = 2 * \pi^2 * \rho * f^2 * (r_m^2) - P_{amb} \quad (3)$$

where,  $P_{thresh}$  is the experimentally determined threshold “negative” pressure for each actinide. Using Eq.2 and Eq.3 together, the radius ( $r_b$ ) for portion of fluid in the radial direction that is above the required  $P_{neg,thresh}$  value can be derived as,

$$r_b = r_m * \left(1 - \frac{P_{neg,thresh} + P_{amb}}{P_{neg,CL} + P_{amb}}\right)^{0.5} \quad (3)$$

Clearly, when  $P_{neg,thresh} = P_{neg,CL}$ , then  $r_b = 0$ . As the rotation frequency “ $f$ ” increases,  $P_{neg,CL}$  increases and so does “ $r_b$ ”. This sensitive radius ( $r_b$ ) is then used to determine the effective sensitive volume ( $V_b$ ) at any  $P_{neg}$  state above the threshold as “ $f$ ” increases. Since both Pu-239 and Pu-240 both exhibit fractional ( $\gamma_i$ ) branch emissions (as listed in Table 1) of alpha particles of different energies,  $V_b$  is calculated as the fraction weighted sum of sub-volumes ( $V_{b,i}$ ) for each of the “ $i$ ” branch emissions, each with its own  $r_{b,i}$ . To illustrate, for a right circular cylinder of radius “ $r = r_{b,i}$ ” and height “ $H$ ”,  $V_{b,i} = \pi * r_{b,i}^2 * H$ . However, the actual shape of the as-manufactured CTMFD’s central bulb comprises for most part, a right circular cylinder with a conical top like shape connected at the end to the two arms (as schematically shown in Fig. 1). These geometrical aspect refinements are taken into account by breaking the CTMFD’s central sensitive volume into several geometric shapes – correcting also for the error in motor speed ( $f$ ) via normal cumulative distribution function value (calculated in the Matlab™ script) wherein the standard deviation equals to the full error (est. ~4%) for  $P_{neg}$  in the motor control.

Once this is done, the predicted count rate ( $C_{pred}$ ) at each  $P_{neg}$  state is then determined by multiplying the experimentally measured full sensitivity count rate ( $C_{fs}$ ), by the aforementioned predicted sensitive volume ( $V_b$ ) which includes contributions to detection from multiple (branching ratio based) alpha emitters (discussed further in Section 2.1), which collectively become progressively involved based on energy each isotope in the mixture. That is,

$$C_{pred} = C_{fs} * V_b \quad (4)$$

where, the full sensitivity activity ( $C_{fs}$ ) is determined by averaging the measured CTMFD count rate at/beyond start of the count rate plateau region [starting at  $P_{neg}$  ( $r_b=0$ ) when  $P_{neg}$  (@  $r_b = \max$ . *SV bulb radius*) the entire central CTMFD bulb volume is now sensitive. Figure 3 shows an example of the predicted versus actually measured count rates in a CTMFD bearing Pu-240 only, wherein, the plateau starts at  $P_{neg} \sim 4.83$  bar.

The above model assumes isotopic homogeneity and neglects 3-D effects. For example, it assumes no variation of  $P_{neg}$  from top to bottom of the sensitive fluid in the central bulb, as well as assumes absence of significant fluid-structure interaction effects at wall-fluid interfaces – esp. when the fluid next to the arms starts to reach  $P_{thresh}$ . Future refinements need to take these aspects into account. As a consequence, some distortion between the predicted and measured detection rates at various  $P_{neg}$  states is to be expected. However, from a practical sense, what is important is to see if the current theoretical framework, and deconvolution algorithm when used with the CTMFD sensor apparatus can accurately assay for the mass/activity fractions of Pu-239 and Pu-240 within the CTMFD fluid mixture.

## 2.2 De-Convolution Algorithm for Pu-239/240 Spectrometry

Using the modeling scheme for predicting detection rate vs  $P_{neg}$  response curves for individual isotopes, as described previously, an algorithm was devised to deconvolute a response curve resulting from an unknown mixture of Pu-239/240 isotopes.

A set of normalized count rate vs  $P_{neg}$  response curves was created for Pu-239:240 mixtures by multiplying the expected (predicted) count rates by the activity ratios of each mixture ranging from 1:0 to 0:1. This is

based on the assumption that the two isotopes remain uniformly mixed and the alpha emissions all contribute to causing CDEs without being interrupted (i.e., negligible spatial separation and wall effects). Figure 4 shows an example of the family of response curves based on experimentally derived  $P_{thresh}$  for Pu-239 and Pu-240 – which include speed control effects. As noted therein, while the dominant alpha energies are well within  $\sim 10$  keV of each other, and the associated recoil nuclei energies are within  $\sim 0.8$  keV of each other, the corresponding  $P_{thresh}$  values are yet separated by  $\sim 0.25$  bar, ranging from  $\sim 4$  bar (for Pu-239) and  $\sim 4.25$  bar (for Pu-240), respectively. The  $P_{neg}$  values are deemed to be accurate to within  $\sim 1-2\%$  (1 SD) error based on the error in rotation frequency (or  $\sim 0.03$  to  $\sim 0.07$  bar). Therefore, the prediction algorithm must also take overall uncertainties into account as well as for subtracting CDEs that may be caused from background radiation (esp., from fast neutrons). It is to be noted that due to the very closely spaced alpha and recoil emissions (Table 1), the response curves derived from the Section 4.1 mathematical model (Fig. 4), even though separated, also involve considerable overlap over the  $P_{neg}$  range of 4.1 bar to 4.9 bar. The dominant Pu-240 recoil energy of 87.596 keV is greater than two of the three alpha recoil energies from Pu-239 emissions. In addition, to arrive at full SV sensitivity even for Pu-239 emissions, the  $P_{neg}$  values range through  $\sim 4.8$  bar. Such closeness and overlaps present a challenge. As such, a suitable algorithm was deemed necessary– one that trains on the mathematical model based response curves of Fig.4, and then deciphers the experimentally obtained response curve data and uncertainties involved, for an arbitrary mixture of Pu-239 and Pu-240; subsequently, to then provide a best-estimate prediction (and uncertainty) for the highest likelihood combination of the two isotopes from a range of possibilities. This methodology is described next.

#### Figure 4

An algorithm was then developed to determine a figure of merit to optimally decipher the highest likelihood of each isotopic activity ratio considered between the two isotopes using the following steps: Note, subscript i indicates a singular Pneg state and subscript r indicates a specific ratio of the two isotopic components within the mixture.

1. The algorithm calculates the difference between the measured count rate and expected (1-D model predicted) count rate for each isotopic ratio (r) at each negative pressure measured.

$$Dif_{i_r} = \left| \frac{CPM_{m_{i_r}}}{AVG(CPM_{m_{i_r}})} - \frac{CPM_{p_{240}_{i_r}}}{AVG(CPM_{p_{240}_{i_r}})} * \frac{X}{(X+Y)} - \frac{CPM_{p_{239}_{i_r}}}{AVG(CPM_{p_{239}_{i_r}})} * \frac{Y}{(X+Y)} \right| \quad (4)$$

where, at any  $P_{neg}$  (i) state for  $i=1,..,n$ ,  $Dif_{i_r}$  is the calculated difference between the measured count rate,  $CPM_{m_{i_r}}$ , and model predicted count rate,  $CPM_{p_{i_r}}$ , for each actinide with X proportion of Pu-240, and Y proportion of Pu-239 e.g. X=1, Y=1, for 1:1 ratio. Note the normalization factor in the denominator of each term is the average of the count rate at the plateau once the entire bulb is sensitive, as described previously.

2. The average difference for each ratio from Eqn. (4) is then calculated by averaging the differences calculated in Step 1 over all Pneg (i) states.

$$Dif_{avg_r} = \frac{\sum_{i=1}^n Dif_{i_r}}{n} \quad (5)$$

where,  $Dif_{avg_r}$  is the average difference for each ratio  $r$ , and  $n$  is the total number of  $P_{neg}$  states measured.

- The measurement error is propagated and similarly averaged as in Step 2 to determine the average error for each ratio as shown below in Eqn. (6).

$$E_{Dif_{i_r}} = \sqrt{\left( \left( \frac{\delta Dif_{i_r}}{\delta CPM_{m_{i_r}}} \right)^2 * (E_{CPM_{m_{i_r}}})^2 + \left( \frac{\delta Dif_{i_r}}{\delta CPM_{p240_{i_r}}} \right)^2 * (E_{CPM_{p240_{i_r}}})^2 + \left( \frac{\delta Dif_{i_r}}{\delta CPM_{p239_{i_r}}} \right)^2 * (E_{CPM_{p239_{i_r}}})^2 + \left( \frac{\delta Dif_{i_r}}{\delta AVG(CPM_{m_i})} \right)^2 * (E_{AVG(CPM_{m_i})})^2 + \left( \frac{\delta Dif_{i_r}}{\delta AVG(CPM_{p240_i})} \right)^2 * (E_{AVG(CPM_{p240_i})})^2 + \left( \frac{\delta Dif_{i_r}}{\delta AVG(CPM_{p239_i})} \right)^2 * (E_{AVG(CPM_{p239_i})})^2 \right)}$$

$$\frac{\delta Dif_{i_r}}{\delta CPM_{m_i}} = \frac{1}{AVG(CPM_{m_i})}$$

$$\frac{\delta Dif_{i_r}}{\delta CPM_{p240_i}} = \frac{-X}{X+Y} * \frac{1}{AVG(CPM_{p240_i})}$$

$$\frac{\delta Dif_{i_r}}{\delta CPM_{p239_i}} = \frac{-Y}{X+Y} * \frac{1}{AVG(CPM_{p239_i})}$$

$$\frac{\delta Dif_{i_r}}{\delta AVG(CPM_{m_i})} = \frac{-CPM_{m_{i_r}}}{AVG(CPM_{m_i})^2}$$

$$\frac{\delta Dif_{i_r}}{\delta AVG(CPM_{p240_i})} = \frac{X}{X+Y} * \frac{CPM_{p240_{i_r}}}{AVG(CPM_{p240_{i_r}})^2}$$

$$\frac{\delta Dif_{i_r}}{\delta AVG(CPM_{p239_i})} = \frac{Y}{X+Y} * \frac{CPM_{p239_{i_r}}}{AVG(CPM_{p239_{i_r}})^2}$$

$$E_{Dif_{avg_r}} = \frac{\sum_{i=1}^n E_{Dif_{i_r}}}{n} \quad (6)$$

4. The standard deviation of the differences for each ratio is then calculated.

$$\sigma_r = \sqrt{\sum_{i=1}^n \frac{(Dif_{ir} - Dif_{avgr})^2}{n}} \quad (7)$$

5. The average error and standard deviation are then summed and divided by the product of the average error and average differences for each ratio. This value is then summed.

$$E_{T_r} = \sigma_r + E_{Dif_{avgr}} \quad E_{sum} = \sum_{r=1}^9 E_{T_r}$$

$$C_r = \frac{E_{sum}}{E_{T_r} * Dif_{avgr}}$$

$$C_{sum} = \sum_{r=1}^9 C_r$$

6. The ratio ( $C_r$ ) is then divided by the sum ( $C_{sum}$ ) in Step 5 to determine the percentage ( $P_r$ ) of confidence responsible for the summed value, and is now indicative of the likelihood for the ratio of components between Pu-239 and Pu-240 to be derived from,

$$P_r = \frac{C_r}{C_{sum}} \quad (8)$$

The above-mentioned algorithm provides for a spectrum of Pr values for any arbitrary mixture of Pu-239 and Pu-240; effectively constituting a figure of merit (FOM) to choose the highest likely (best estimate) value for the ratio of these two isotopes and the associated uncertainty as discussed in Section 4.2.

### 3. Protocol for Sample Preparation for CTMFD based Alpha Spectroscopy

The study was based on certified Pu-239 and Pu-240 “standards” supplied by U.S. National Institute of Standards and Technology (NIST) and Eckert & Ziegler Isotope Products Technical Service (EZIPTS). Tables 2 and 3 present pertinent data from these two certified isotope standard source suppliers. Utilizing expensive “standards” directly from the regulators and federally recognized agencies, allowed us to validate for the accuracy of TMFD based prediction results, without having to re-certify the accuracy of samples used in our studies against predictions from mass spectroscopy (MS) type techniques. As noted earlier, conventional alpha spectrometry techniques based on PIPS and LS cannot discern between the (< 10 keV separated) alpha emissions from Pu-239 and Pu-240.

**Table 2. NIST Supplied Technical Data for Pu-239 Sample**

Pu-239 Sample Activity	38.41 Bq/g (in 2.77 g vial) in 3.7M HNO <sub>3</sub>
Uncertainty	0.46% (2 SD)
Solution Density	1.108 g/mL at 23.9°C
Pu-240 Activity (as of 11/9/1999)	0.002 Bq/g
Pu-241 Activity (as of 11/9/1999)	0.02 Bq/g

Am-241 Activity (as of 11/9/1999)	0.001 Bq/g
-----------------------------------	------------

**Table 3. EZIPTS Supplied Technical Data for Pu-240 Sample (in 1M HNO<sub>3</sub> vials)**

Nuclide	Atom%	Total Activity%	α-Activity%
Pu-238	0.00678	0.334	0.509
Pu-239	0.735	0.132	0.201
Pu-240	98.861	65.135	99.285
Pu-241	0.1146	34.396	n/a
Pu-242	0.283	0.00325	0.00496

Notes:

- (1) Isotopic compositions provided by Oak Ridge National Laboratory
- (2) Am-241 = 0.0757% (of Pu-240) on 6/3/2010
- (3) Pa-233 =  $7.58 \times 10^{-3}$ % of Pu-240 on 6/3/2010
- (4) Sample Activity ~ 7 Bq/mL in 1M HNO<sub>3</sub>

As noted from Table 2, the NIST-supplied source of Pu-239 was almost 100% Pu-239 with very low level of contamination of other alpha emitters. However, we see from Table 3 that the Pu-240 sample comprised ~34.4% activity from Pu-241 with a half-life of ~13y, and which decays via beta decay to Am-241 (an alpha emitter). Considering the experiments for this study were conducted during 2020-2021 time frame, after a lapse of about 10y, a significant buildup of Am-241 activity (comprising about 10-15% of alpha activity) must be accounted for. This was indeed taken into account as discussed below.

### 3.1 Extraction of Pu-239 and Pu-240 from nitric acid based vials & Rejection of Am-241 Contamination

The engineered fluid decafluoropentane (DFP) with the molecular formula C<sub>5</sub>H<sub>2</sub>F<sub>10</sub> [rated (0/0/0) for flammability/health/instability on the U.S. National Fire Protection Association (NFPA) standard], and density = 1.6 g/mL was used as the primary working fluid for detection of incident radiation in the CMTFD with a 16 mL sensitive bulb system used for the studies reported in this paper. Since HNO<sub>3</sub> is not soluble in DFP, the as supplied Pu in HNO<sub>3</sub> needed to be extracted for transfer into DFP. This required the use of a suitable extraction procedure from the stock nitric acid solution into the CMTFD working fluid which preferentially transferred only the Pu isotopes but not the Am isotopes.

For this procedure (illustrated in Fig. 5), a microliter Eppendorf™ pipette (accurate to  $< \pm 0.8\%$ ) was used to dilute the certified plutonium sample into 6 mL of nitric acid solution. Since nitric acid is not miscible in DFP, tributyl phosphate (TBP) was used to first extract the plutonium from the nitric acid solution into DFP. A mixture was created consisting of 4 mL DFP and 2 mL TBP and then combined with the diluted plutonium bearing stock solution. This mixture was shaken vigorously for thirty seconds and allowed to settle for thirty minutes. While the mixture settles, the TBP preferentially extracts the plutonium from the nitric acid after which it is transferred into the DFP and then into the CMTFD, as shown in Fig. 5. We have previously demonstrated and as is also well-known that the extraction efficiency of TBP for Am isotopes is negligible;  $< 4\%$  [9, 13]. Therefore, at most the Pu-240 bearing sample could at most comprise  $< 4\%$  of 10% or  $< 0.04\%$  of total alpha activity in the Pu-240 extracted sample. Also, a cross-check was put in place based on considering that the E<sub>α</sub> for Am-241 is ~ 5.5 MeV vs about 4.25 MeV for Pu-240 and 4.0 MeV for Pu-239. This provides a secondary check for the presence or absence of Am-241 contamination. The

1  
2  
3 higher the value for  $E_{\alpha}$ , the lower is the  $P_{neg}$  state required for detection in the CTMFD. If significant Am-  
4 241 activity were present, this would very readily manifest itself with detection onset for  $P_{neg}$  states well  
5 below 4 bar (towards  $\sim 3$  bar). We note from Fig. 3 that  $P_{thresh}$  for the Pu-240 based sample occurs only  
6 at/around  $P_{neg} \sim 4.25$  bar with no detection activity below 4.25 bar. This served as an extra check that the  
7 extraction protocol as used predominantly ( $>99.5\%$ ) transfers only the Pu-240 isotope for the CTMFD  
8 based studies reported in this paper.  
9

10  
11  
12 *Fig. 5*  
13

14 After thirty minutes, the entire mixture was diluted in 94 mL DFP and poured into a titration funnel. Due  
15 to density differences, the nitric acid forms a layer at the top while the DFP/TBP (now containing the  
16 extracted actinide) settles into the bottom layer. The actinide laden DFP/TBP was then gravimetrically  
17 separated and stored in a 125 mL Nalgene™ bottle. This process builds upon the well-established procedure  
18 used worldwide for the plutonium-uranium extraction (PUREX) process and our past studies have  
19 demonstrated excellent, reproducible extraction efficiency for Pu isotopes, and  $< 4\%$  for Am-241 [10].  
20  
21  
22

23 *Fig. 6*  
24  
25  
26

### 27 3.2 Preparing CTMFD apparatus for Alpha Spectroscopy

28 After extraction, as noted in Fig. 5, the DFP/TBP mixture (now containing the plutonium isotopes) was  
29 transferred into the CTMFD glassware through a  $0.2 \mu\text{m}$  PTFE filter (a process that takes about 1-min.,  
30 evacuated of air, and sealed with a rubber stopper. As to be expected of all fluids, the sensing fluid within  
31 the CTMFD contained non-condensable gases (air) which can lead to false CDEs, and must be degassed –  
32 an aspect that is readily achieved either via ultrasonic bath submersion or via use of an external neutron  
33 source such that about 20+ CDEs are sequentially induced when the CTMFD is operated at up to  $P_{neg} \sim 5$   
34 bar. Each CDE leads to progressive release of dissolved gases. A protocol was developed using a 10 mCi  
35 Am-Be isotope neutron source (emitting  $\sim 2 \times 10^4$  n/s) about 1 m away from the CTMFD, which leads to  
36 CDEs within 1-10s for each cavitation event. The accumulated air within the CTMFD's cavity space in the  
37 upper arms is then removed via syringe and the CTMFD is now sealed and ready for alpha spectroscopy  
38 within  $\sim 10$  min. from start.  
39  
40  
41

42 CDEs in a degassed CTMFD can occur also due to external neutron background and must be ascertained  
43 for subtraction/correction. It was found that during the course of the data acquisition for this paper, without  
44 any intentionally entered alpha bearing isotope within the 16 mL CTMFD filled with vendor-supplied  
45 filtered DFP, our Lafayette, IN, USA laboratory based neutron background (from cosmic and other isotope  
46 neutron sources in storage cabinets) led to a background count rate ranging from  $\sim 0.33$  cpm at  $P_{neg} \sim 4$  bar,  
47 towards  $\sim 0.55$  cpm at  $P_{neg} \sim 5.5$  bar. Figure 6 shows such a typical background detection rate vs  $P_{neg}$  state  
48 variation. The background CDE rate (in a degassed system) is first estimated with the CTMFD filled with  
49 only DFP fluid (i.e., without alpha emitters). Thereafter, the same CTMFD is refilled with DFP containing  
50 various extracted ratios of Pu isotopes and the aggregated cpm values are corrected for each of the  $P_{neg}$   
51 states for conducting alpha spectrometry. It is expressly assumed (and reasonable care was taken) that the  
52 neutron background (including cosmic neutrons) in the experiment room remained unchanged during the  
53 course of alpha detection experiments. This was verified at start and end of data acquisition for each  
54 campaign.  
55  
56  
57  
58  
59  
60

As an extra note, to ensure consistent operation (within +/- 10% of the calibration curve), prior to start of data acquisition, the specific CTMFD unit's detection efficiency vs  $P_{neg}$  is compared to its calibration curve generated for that unit with an Am-Be source, right after fabrication and readiness for use.

#### 4. Results of Experiments and Data Analyses

This section presents results of experiments and analyses conducted with Pu-239: Pu-240 ratios varying between, 1:1, 0:1, 5:1, and 1:1. For each response curve, the raw cpm data are background corrected and then normalized to the detection rate after reaching the plateau region. For example the background subtracted cpm values are normalized by 1.4 cpm in the example shown in Fig. 3 for a Pu-239:Pu-240 ratio of 0:1. Note: this example case illustrates results obtained with only ~ 0.02 Bq total Pu-240 activity in the 16 mL sensitive volume CTMFD.

##### 4.1 Experimentation and results for various Pu-239:Pu-240 ratios

For the results presented in subsequent figures, data were obtained with ~ 0.1 Bq total activity in the sensitive volumes. Error bars represent 1 SD uncertainty.

Figures 7-10 present the normalized cpm vs  $P_{neg}$  data response curves for the four Pu-239:Pu-240 activity ratios, ranging from 1:0 to 0:1. Cavitation detection events in the CTMFD system are monitored and timed using infrared sensors,  $P_{neg}$  states are dynamically controlled with temperature compensation, and CDEs are recorded using LabVIEW virtual instruments software. Figs. 7-10 show the detector response overlaid with the best-fit model (predicted) curves. As expected, the background subtracted response of the CTMFD is initially zero below the negative pressure threshold,  $P_{thresh}$ , for the specific actinide (e.g., ~4.0 bar for Pu-239). When the detector approaches the threshold, the actinide decay at the centerline of the bulb is now able to be detected. As the  $P_{neg,cl}$  increases, the  $P_{neg,thresh}$  pressure state expands radially away from the centerline and progressively causes actinides located to that radius to also participate in the detection process until the entire bulb is  $\geq P_{neg,thresh}$ . Despite the occasional departure between the 1-D model prediction vs actual data, the response spectra correlate reasonably well overall.

*Figures 7-10.*

##### 4.2 Data Analysis

The response curve data for figure of merit versus the model predictions were analyzed using the deconvolution algorithm discussed in the previous section and the results are depicted graphically in Figures 11 through 14 for the value of the error propagated normalized probability,  $P_r$  (%), versus possible Pu-239 content in a Pu-239/Pu-240 mixture. Results are also summarized in Table 4. Figs. 11-14 also include the predicted spectroscopy data for alpha activity vs energy for each of the four mixture configurations.

As noted from Table 4, the correct Pu-239:Pu-240 activity ratio is accurately predicted for all the experiments by a good level of confidence; thereby, indicating the overall uncertainty of the prediction to be within ~ +/-12 % of the activity ratio, based on the cases considered.

**Table 4. Summary of Expected vs Measurement-based Predictions for 4 Test Cases (Pu-239:Pu-240 Activity Content in Mixtures)**

Case # (Pu-239:Pu-240Ratio)	Expected (NIST-Std. Based)	Predicted - Most Likely**

	<b>% (*) Pu-239:Pu-240</b>	<b>% (±) Pu-239 : Pu-240</b>
1 (1:0)	100 : 0	97 : 3 (±12)
2 (0:1)	0 : 100	0 : 100 (±5)
3 (1:1)	50 : 50	44 : 56 (±12)
4 (5:1)	83 : 17	83 : 17 (±9)
(*) ~1.5% est. total sample activity uncertainty = ~0.5% (NIST std.) + ~1% (Pipetting-Transfer)		
(**) – Algorithm based highest probability FOM – See Figures 11-14		

*Figures 11-14.*

## 5. CTMFD Attributes for Alpha Spectrometry - Overview

An overview of the type of CTMFD apparatus used for the present study and its key attributes for high resolution alpha spectrometry are summarized in Table 5. The interested reader with expertise in the field can draw her/his own conclusions in terms of comparison against alternate technologies.

<b>Parameter</b>	<b>Value / Discussion</b>	<b>Notes</b>
Sensitivity (alpha/fission detection efficiency)	95%+ (Note: this is offered in $4\pi$ )	Determined to +/-5% of NIST certified source activity
Alpha Energy Range	~1.8-9 MeV	Tested using U, Pu, Am, Cm, Rn-Po and B(n, $\alpha$ )Li
Energy resolution achieved	~1.4 keV	Recoil energy difference of alpha emissions from Am-241 and Pu-238
Tested Alpha-fission sample activity levels	~ $10^{-3}$ Bq/mL	Based on ~15 mL CTMFDs and $\leq 60$ s (average time) between detection events.
Minimum detection level limit	Practically attainable lower limit is undetermined as yet – will depend on combination of variables – see notes column.	Varies inversely with SV size, counting time available, and neutron background suppression.
Rejection of background gamma-beta radiation	100%	Tested through $10^4$ R/h environments and for Pneg < 25bar.
Sample preparation time for start of alpha spectroscopy and isotope ratio.	45-60 min.	Starting with aqueous sample to transfer into CTMFD ready for counting – Figure 5.

Final Accepted Version— per Peer Review (Rusi Taleyarkhan → JAAS ; 7.Dec.2021)

Impact of foreign particulates gases, and possibility of color quenching; e.g., from environmental samples	False CDEs due to impurities are overcome with as-used sample preparation protocol; No influence of color.	Filtration through 0.2 $\mu\text{m}$ PTFE filter followed with degassing; alternately, via precompression [14].
Intrinsic neutron detection efficiency (%)	25% to 80% (care must be taken to determine and correct for neutron background CDEs)	Varies with SV size (15 mL to 80 mL) – tests with Cf-252 fission neutron spectrum
Detection fluid types (typical)	DFP, Acetone, Methanol	DFP is preferred and currently used as baseline for both alpha, fission and neutron spectroscopy; may be borated for enabling fast+epithermal neutron spectroscopy.
Form factor (typical)	0.2m (OD) x 0.3m (H)	Can accommodate SV sizes ranging from 0.5mL towards 100 mL within same overall form factor.
Weight	3-5 kg	Varies with SV
Power	50 W (DC) or ~1 kW (AC)	Power estimates are for either DC or AC drives.
Operation control-data acquisition and analysis.	Remote-Wired/Wireless-Automated; Background & Temperature compensated.	LabView software and Arduino based; PC or PDA based.

## 6. Summary and Conclusions

This article discusses a novel, rapid, wet chemistry technique for spectroscopically detecting trace ( $< 10^{-3}$  Bq/mL) level alpha emitting radionuclides with under 10 keV alpha energy resolution. The CTMFD sensor technology was utilized and assessed for the ability to decipher trace level Pu-239 and Pu-240 content in mixtures of these two isotopes ranging in alpha activity content from 1:0 to 0:1 in relative proportions.

For the work presented in this paper, a rapid ( $< 1\text{h}$ ) extraction-transfer protocol was developed to create DFP sensing fluid mixture quantities of these isotopes for CTMFD based examination and to derive the mixture's characteristic response function, viz., alpha decay detection rate over a range of tensioned metastable state negative pressure (*P<sub>neg</sub>*) states ranging from 4.0 bar for Pu-239, to about 4.25 bar for Pu-240. An accompanying methodology and error propagation algorithm were developed to analyze-deconvolute the mixture's response curve comprising the Pu alpha emitting isotopes, and to derive the likely composition of each isotope within the mixture. For each of the four Pu-239: Pu-240 activity ratios: 1:0, 5:1, 1:1 and 0:1, the algorithm correctly predicted the most likely ratio compositions for the two Pu isotopes. Overall, the results from the experiments revealed this technique to be capable of enabling Pu-239:Pu-240 mixture spectroscopy with an estimated uncertainty of  $\pm 5\%$  to  $\pm 12\%$ ; that is, via enabling the accurate ( $\sim 90\%$ ) classification of each mixture composition tested in all experiments, which then translates into prediction of the spectroscopic alpha energy emission activity for the mixture.

It is noteworthy that, the CTMFD based approach discussed in this paper enables such identification of the Pu-239:Pu-240 ratios from 1:0 to 0:1 with uncertainty ranging from 5% to 12%, within  $\sim 3\text{-}4$  h of counting

for any arbitrary ratio, inclusive of sample preparation and data acquisition from a single pre-calibrated CTMFD. As a side note, it is pointed out that the 5:1 activity ratio case actually translates into a mass ratio of ~20:1 due to the ~4x higher half-life for Pu-239 (~24,390 y) vs Pu-240 (6,580y). This enablement would appear suitable for nuclear forensic applications such as for identifying the source/origin of the Pu-based SNM as well as for environmental samples.

### Acknowledgements

This research was sponsored with funding from the Laboratory Directed R&D program of Savannah River National Laboratory, the U. S. Department of Energy / Nuclear National Safety Administration, the U. S. Nuclear Regulatory Commission Fellowship, and in part by Purdue University, State of Indiana. The authors are grateful for the assistance from various colleagues (past and present) at Purdue University and SRNL. We wish to acknowledge the assistance from Purdue University's REMS organization.

### References

- [1] P. W. Krey, B. T. Krajewski, HASL, 249, pp.1-67 (1972).
- [2] G. Knoll, "Radiation detection and measurement," 3<sup>rd</sup> Ed. John Wiley & Sons, Inc., (2000).
- [3] R. E. Perrin, G. Knobeloch, W. Armijo, D. Efur, Intl. J. Mass Spectrometry Ion Proc., 64 (1975) 17.
- [4] V. E. Noshkin, C. Gatrousis, Earth Planet. Sci. Lett., 22, 111 (1974)..
- [5] S. P. LaMont, S. E. Glover, R. H. Filby, "Determination of plutonium-240/239 ratios in low activity samples using high resolution alpha spectrometry," J. Radioanalytical and Nuclear Chemistry, Vol. 234, Nos.1-2, 195-199 (1998).
- [6] A.S.Bon, E. Bond, M.Croce, T.Holesinger, T. Kunde, G. Rabin, ..J. Ullom, "Measurement of the 240Pu/239Pu mass ratio using a transition-edge-sensor microcalorimeter for total decay energy spectroscopy," Analytical Chemistry, 97(7), 3996-5000, (2015).
- [7] R.P. Taleyarkhan, J.R. Lapinskas, Y. Xu "Tensioned metastable fluid detectors and nanoscale interactions with external stimuli – theoretical-cum-experimental assessments and nuclear engineering applications," *Nucl. Engr. Design*, Vol. 238 pp. 1820-1827 (2008).
- [8] R. P. Taleyarkhan, J. Lapinskas, B. Archambault, J. Webster, T. Grimes, A. Hagen, K. Fischer, S. McDeavit, and, W. Charlton, "Real-time monitoring of actinides in chemical nuclear fuel reprocessing plants," *Chemical Engr. Research and Design*, Vol. 91, pp. 688-702 (2013).
- [9] M. Hemesath, N. Boyle, B. Archambault, T. Lorier, D. DiPrete, R. P. Taleyarkhan, "Actinide in air (Rn-progeny rejected alpha spectroscopy with tensioned metastable fluid detectors," *Journal of Nuclear Engineering and Radiation Sciences* (In-Press), (2021).
- [10] R. P. Taleyarkhan, "Monitoring neutron radiation in extreme gamma/x-ray radiation fields," *Sensors* 2020, Vol. 20, 640; doi:10.3390/s20030640, 11 pages. [www.mdpi.com/journal/sensors](http://www.mdpi.com/journal/sensors), (2020).
- [11] R. P. Taleyarkhan, B. Archambault, A. Sansone, T. Grimes, A. Hagen, "Neutron spectroscopy and H\*10 dosimetry with tensioned metastable fluid detectors," *Nucl. Instr. & Meth. In Phys.Res., A* Vol. 959, No. 163278 (2020).
- [12] B. Archambault, A. Hagen, T. Grimes, and R. P. Taleyarkhan, "Large-array special nuclear material sensing with tensioned metastable fluid detectors," *IEEE Sensors Journal, Special Issue*, Vol. 18, No.19, (2018), pp. 7868-7874. <http://dx.doi.org/10.1109/JSEN.2018.2845344>. Accessed Oct. 19, 2020.
- [13] P. C. Doto, L. E. Burns, and, W. W. Schulz, "Solvent extraction process for recovery of americium-241 at Hanford," *Am. Chem. Soc. Symp. Series*, Vol. 161, Chap. 7, pp 109-129 (1981).
- [14] R. P. Taleyarkhan, J. A. Webster, A. Sansone, B. Archambault, R. Reames, and C. D. West, "Metastable liquid cavitation control (with memory) apparatus, methodology and results: for radiation

Final Accepted Version– per Peer Review (Rusi Taleyarkhan → JAAS ; 7.Dec.2021)

1  
2  
3 detection, reactor safety and other industrial applications,” *Journal of Nuclear Engineering and Radiation*  
4 *Science*, Vol.3/011004-1 to 10, Vol.3, January, 2017.  
5  
6  
7  
8  
9  
10  
11  
12  
13  
14  
15  
16  
17  
18  
19  
20  
21  
22  
23  
24  
25  
26  
27  
28  
29  
30  
31  
32  
33  
34  
35  
36  
37  
38  
39  
40  
41  
42  
43  
44  
45  
46  
47  
48  
49  
50  
51  
52  
53  
54  
55  
56  
57  
58  
59  
60

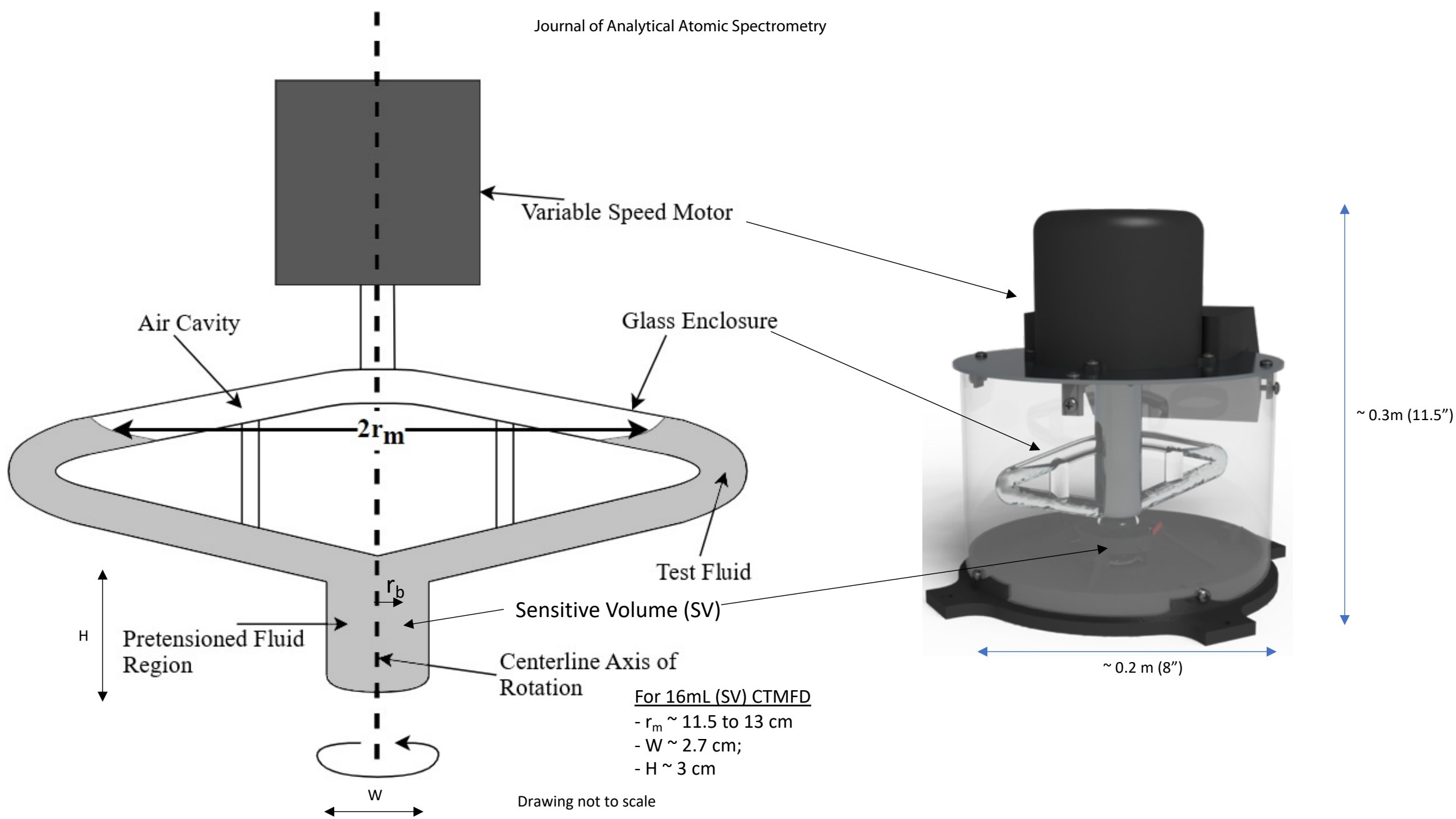


FIG.1 16 ML Sensitive Volume (SV) CTMFD – Schematic (L) & Pictorial (R)

1  
2  
3  
4  
5  
6  
7  
8  
9  
10  
11  
12  
13  
14  
15  
16  
17  
18  
19  
20  
21  
22  
23  
24  
25  
26  
27  
28  
29  
30  
31  
32  
33  
34  
35  
36  
37  
38  
39  
40  
41

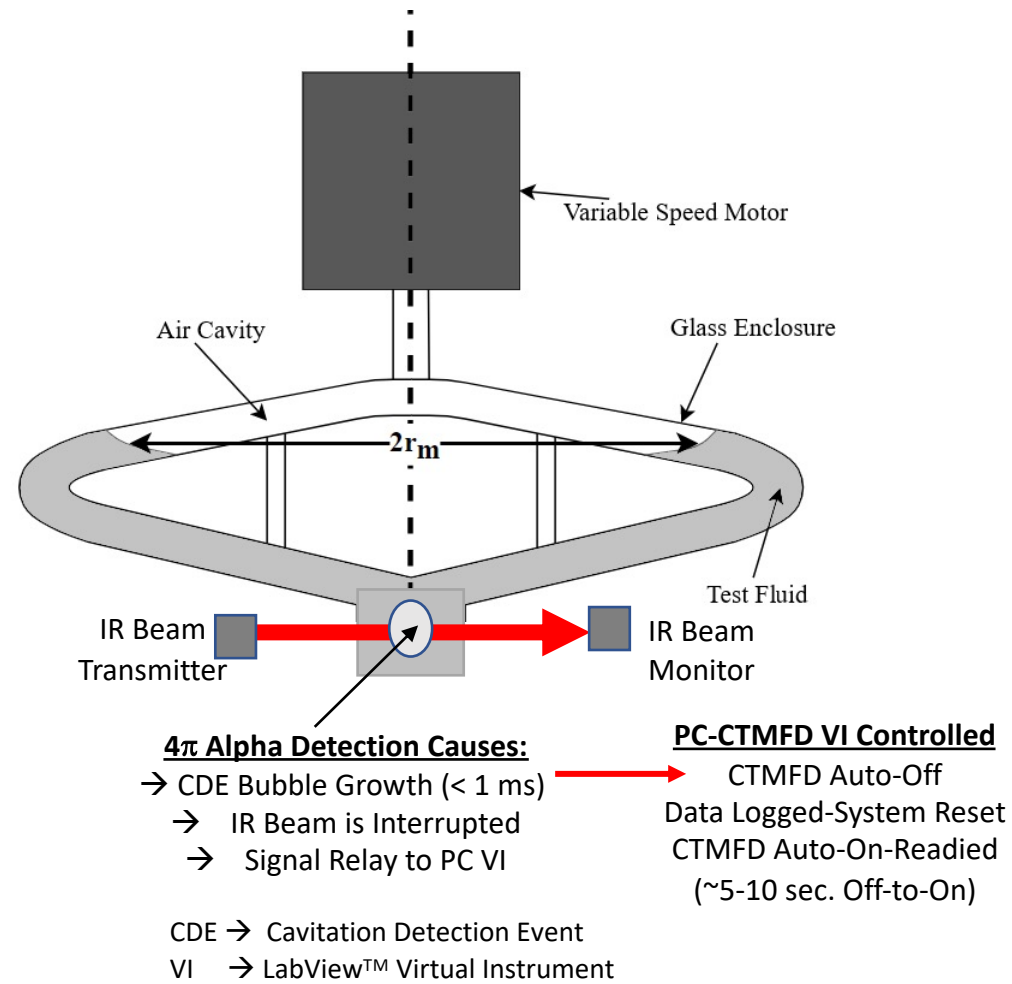


FIG. 2. CTMFD 4p Alpha Detect-Record-Control System Schematic

### Comparison of Measured vs Modeled Count Rates

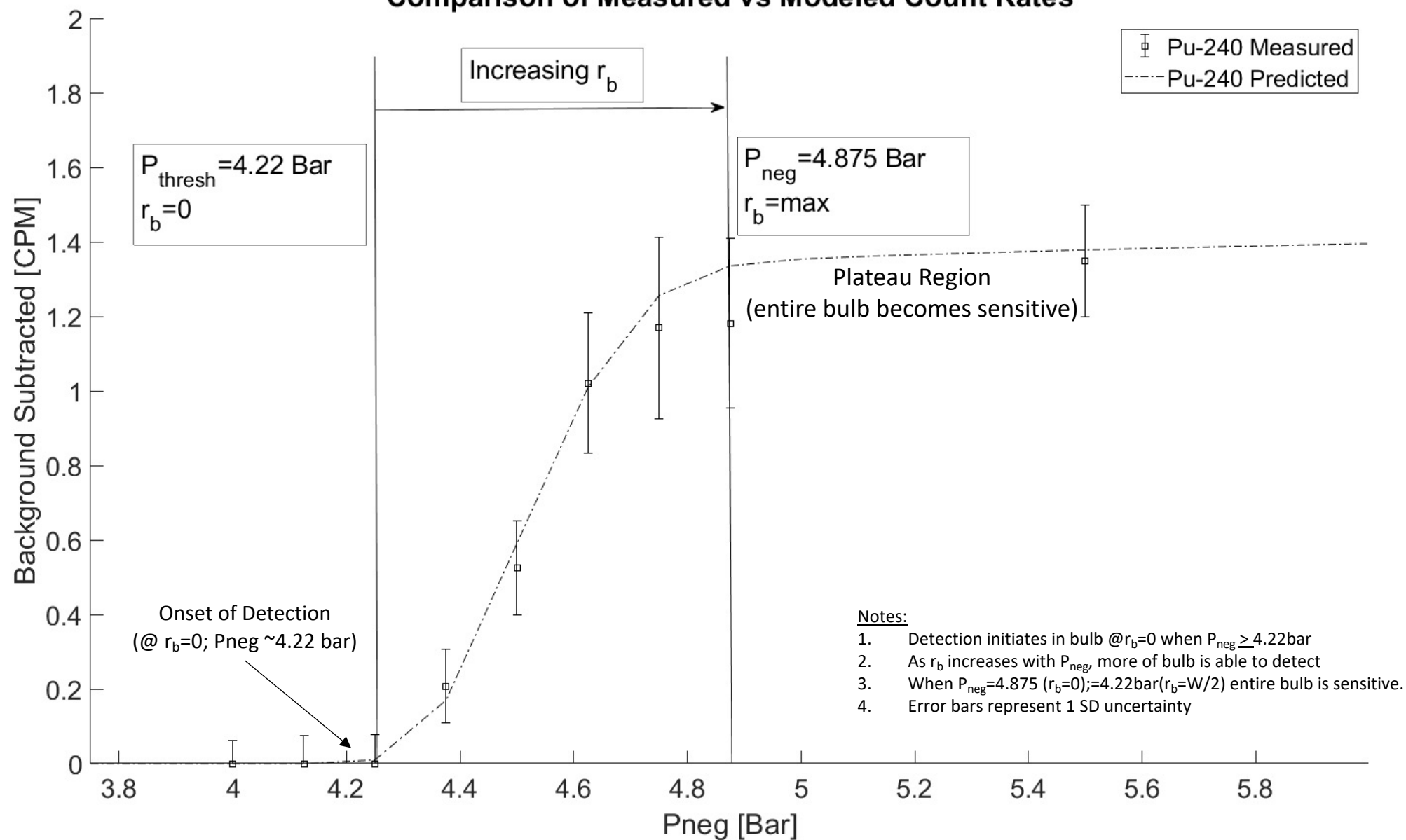


FIG. 3 Model Illustrative Example– Variation of measured count rate vs Pneg for Pu-240 using 15cc CTMFD

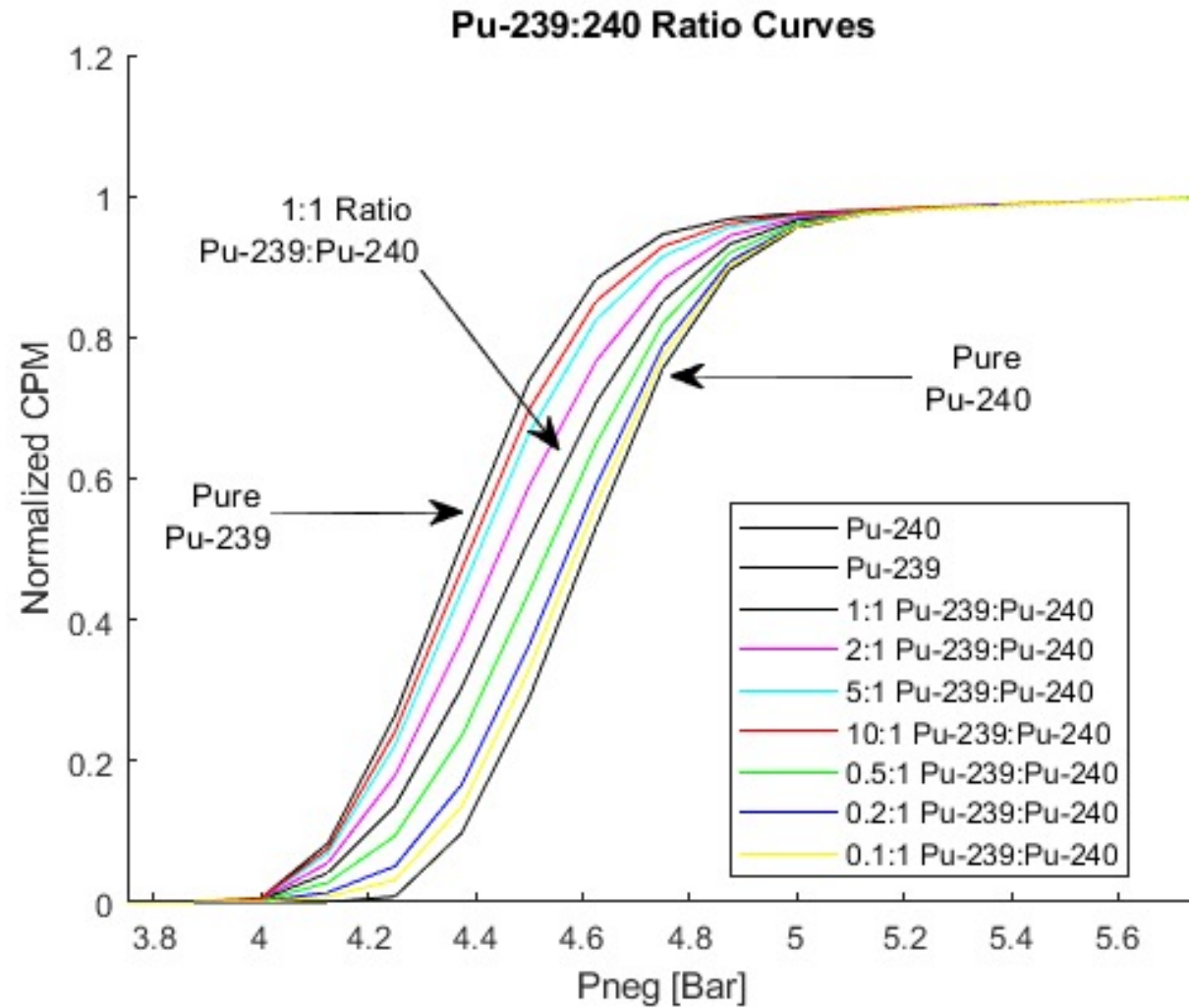
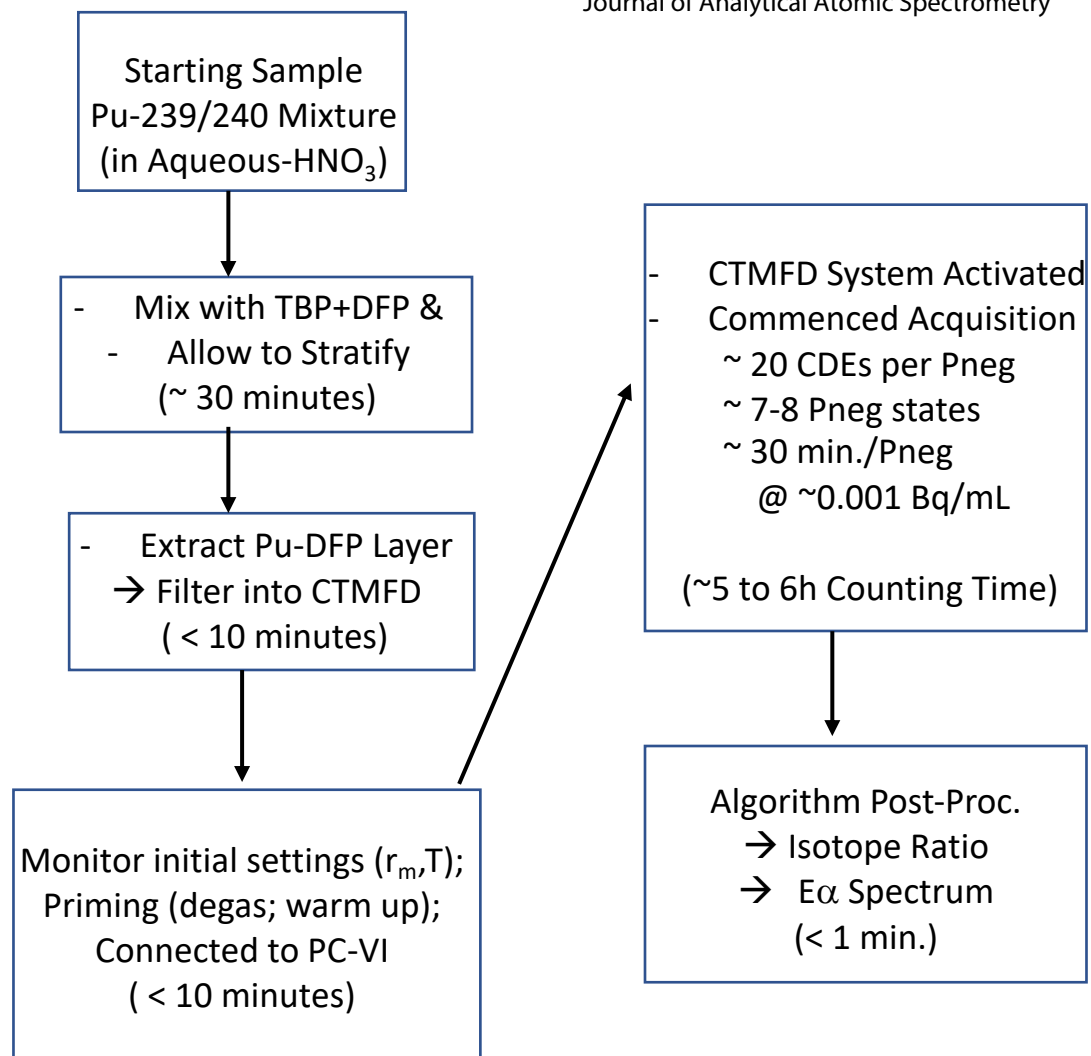


FIG. 4 Theoretical model based template for count rate vs  $P_{neg}$  for various Pu-239:Pu-240 activity ratio mixtures



## Notes:

- 1) ~100%  $4\pi$  alpha detection efficiency (vs NIST standards)
- 2) 15 mL CTMFD sensitive volume used for this study
- 3) ~0.002 Bq/mL corresponds to Fig. 3 example
- 4) Lower specific activity samples\* → longer counting times.
- 5) Upon mixing sample, Pu-DFP-TBP layer settles to bottom
- 6) Filtration is usually via 0.2  $\mu\text{m}$  PTFE filter caps
- 7) Degassing via repeated CDEs with Am-Be neutron source
- 8) Background count rate corrected  
(either by testing w/o actinide beforehand or via separate CTMFD w/o actinide)

(\*) - or compensate with CTMFD SV > 15 mL

FIG. 5 Steps & Approximate Times Involved in Pu-239:Pu-240 Ratio & Alpha Spectroscopy with CTMFD

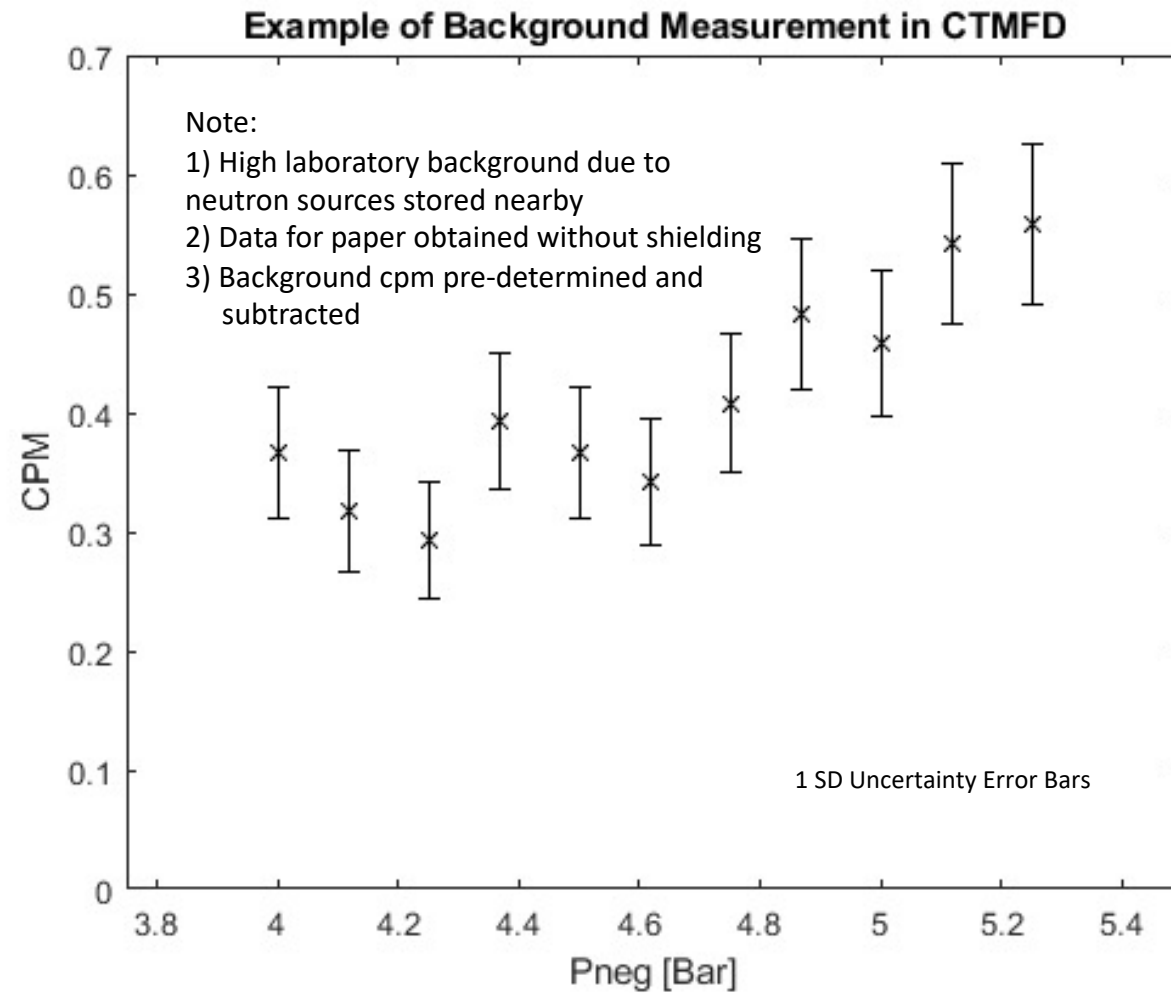


FIG. 6 Background variation of count rate vs  $P_{neg}$  using 15cc CTMFD

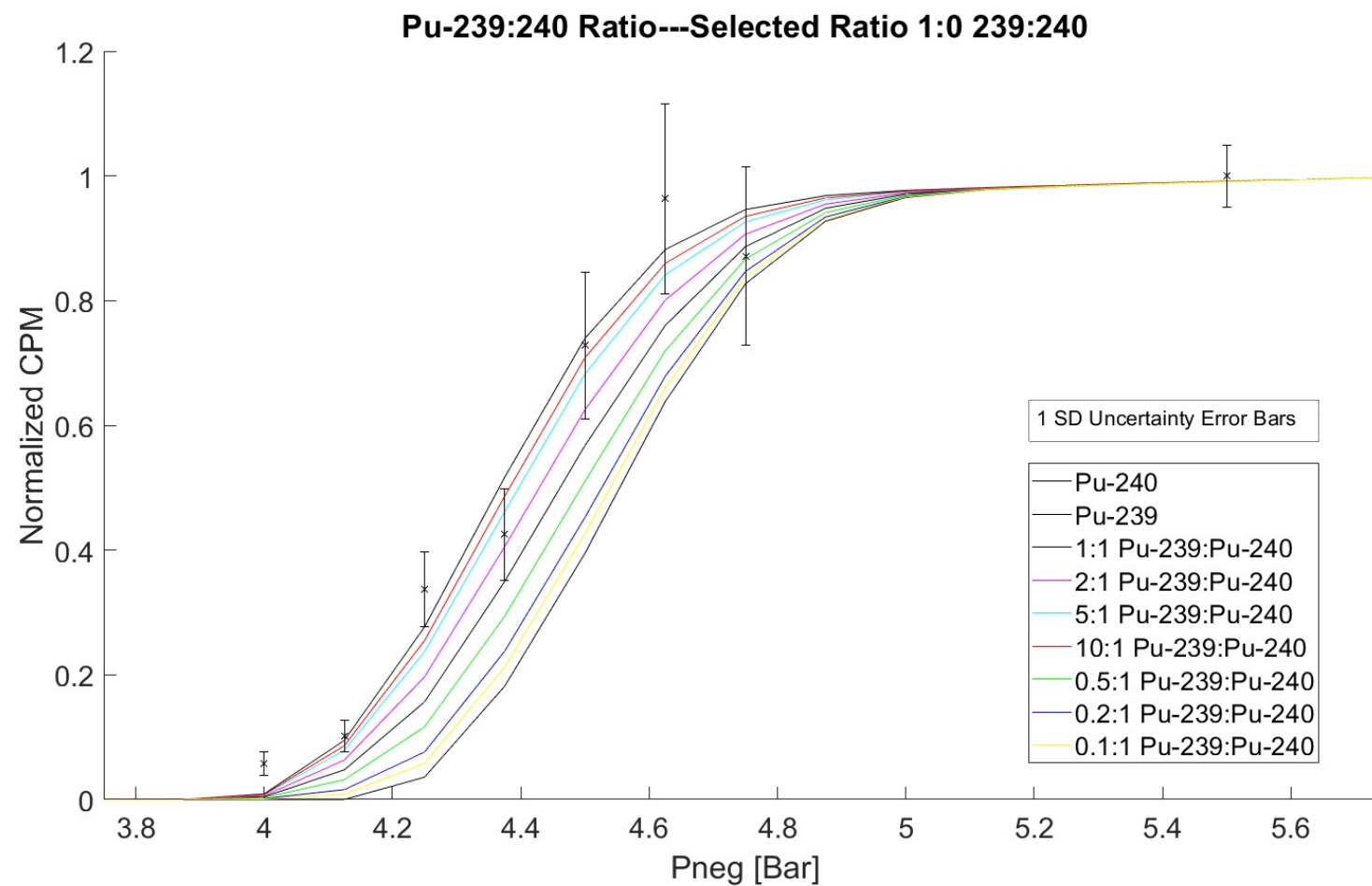


FIG. 7 Variation of normalized count rate vs Pneg for Pu-239:Pu-240 = 1:0 activity ratio mixture

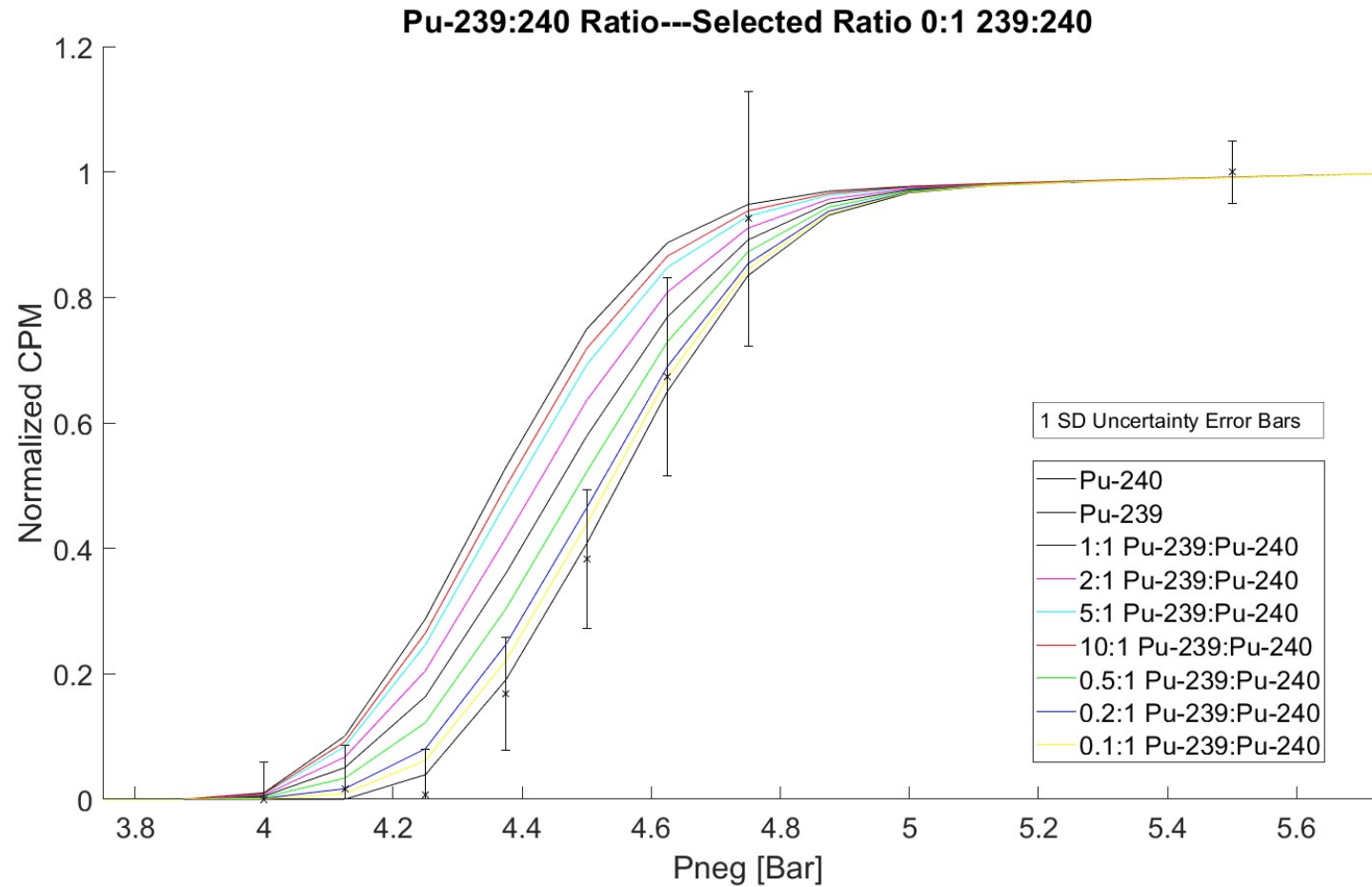


FIG. 8 Variation of normalized count rate vs Pneg for Pu-239:Pu-240 = 0:1 activity ratio mixture

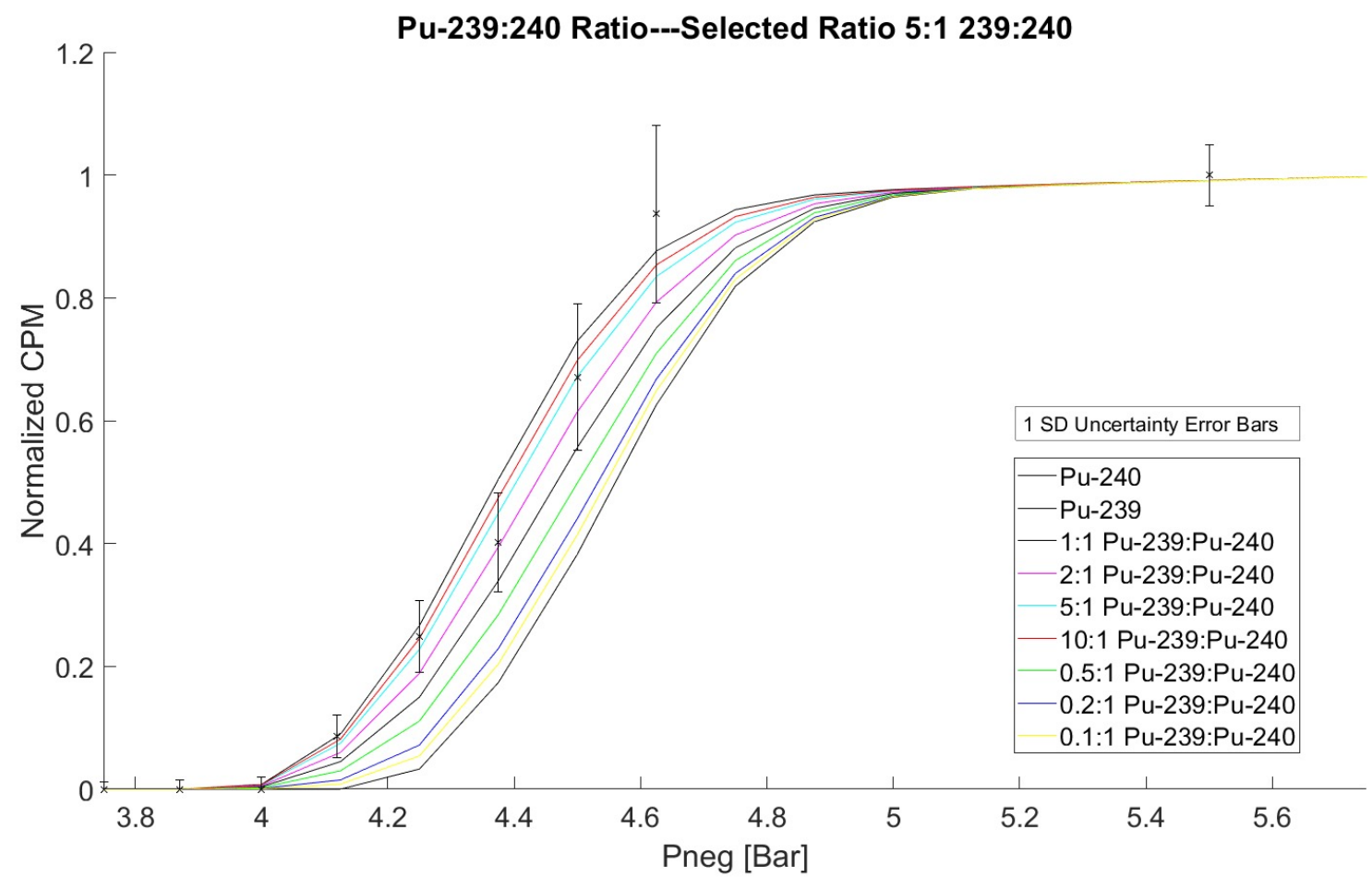


FIG. 9 Variation of normalized count rate vs Pneg for Pu-239:Pu-240 = 5:1 activity ratio mixture

1  
2  
3  
4  
5  
6  
7  
8  
9  
10  
11  
12  
13  
14  
15  
16  
17  
18  
19  
20  
21  
22  
23  
24  
25  
26  
27  
28  
29  
30  
31  
32  
33  
34  
35  
36  
37  
38  
39  
40  
41

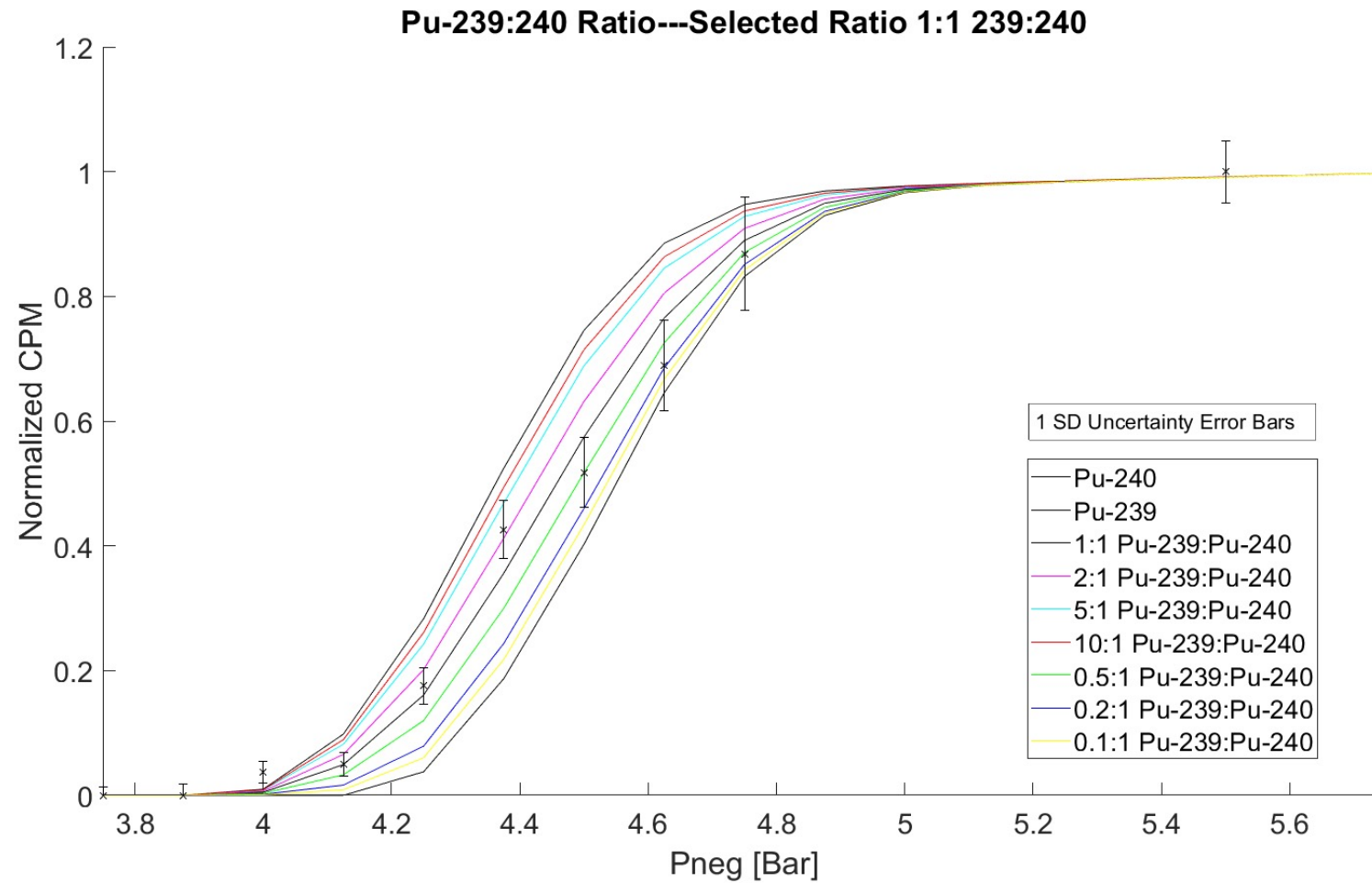


FIG. 10 Variation of normalized count rate vs Pneg for Pu-239:Pu-240 = 1:1 activity ratio mixture

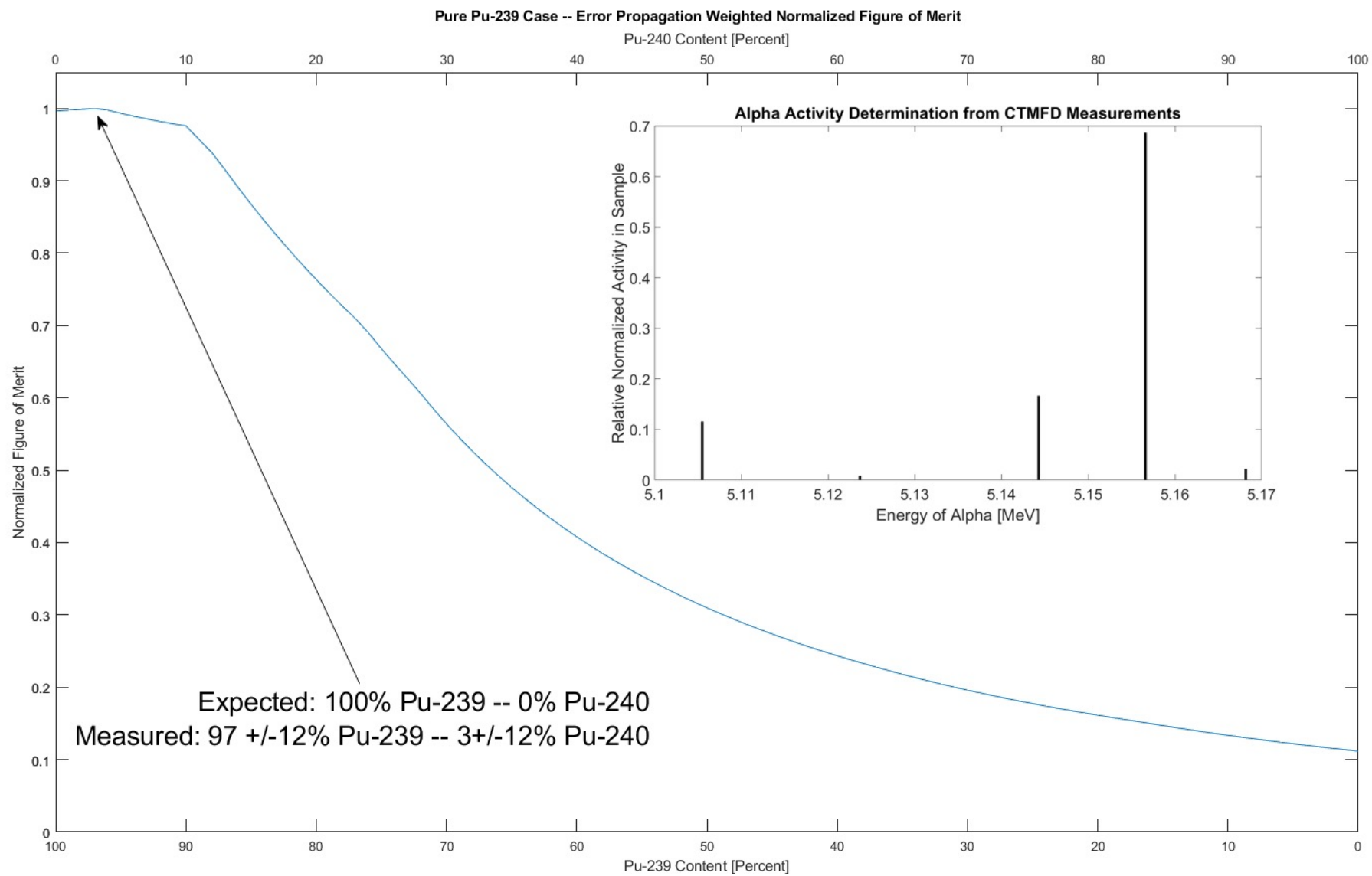


FIG. 11 Variation of FOM for 1:0 Activity Ratio (100% Pu-239; 0% Pu-240) & Predicted Alpha Energy Spectrum

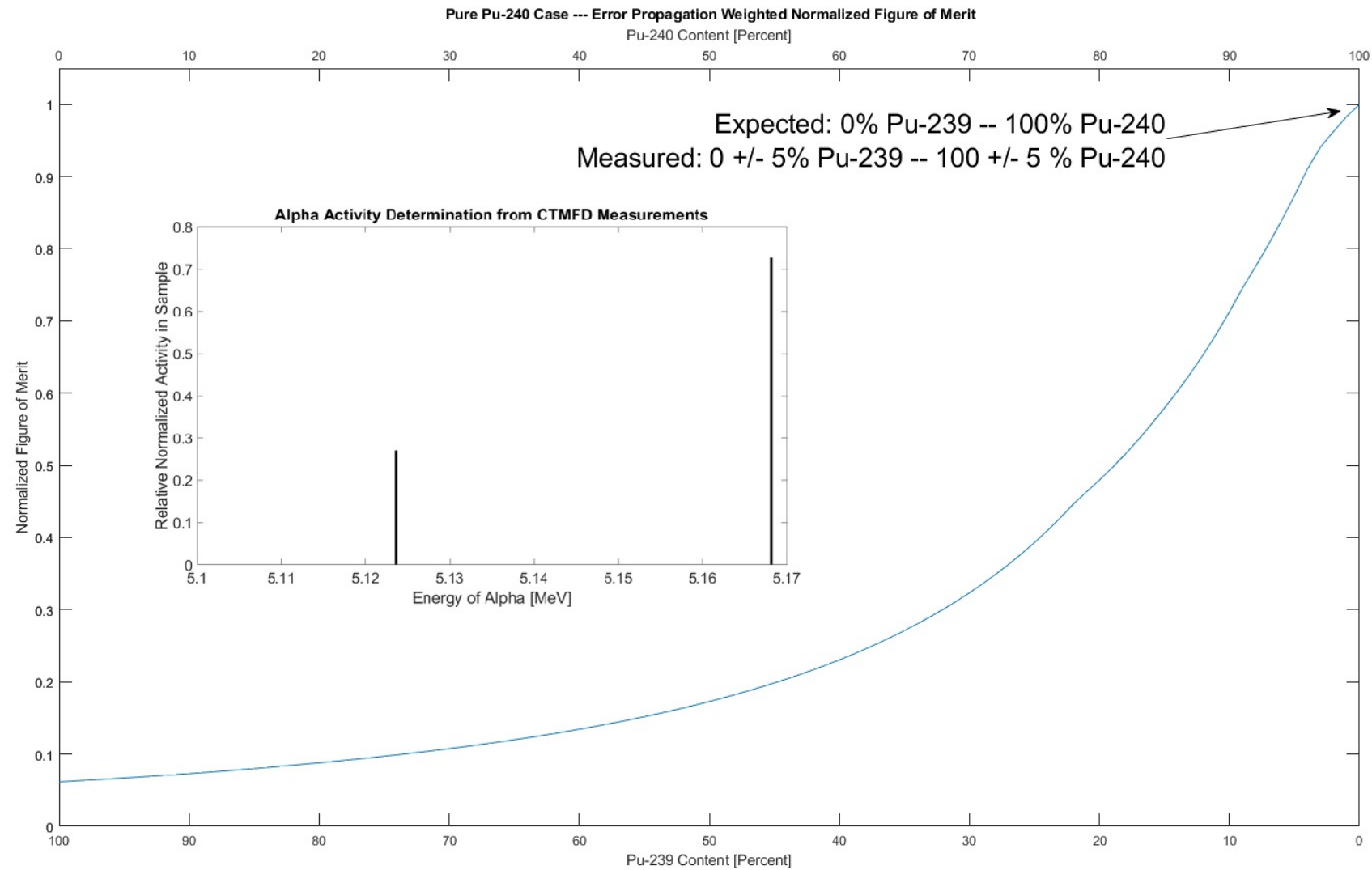


FIG. 12 Variation of FOM for 1:0 Activity Ratio (0% Pu-239; 100% Pu-240) & Predicted Alpha Energy Spectrum

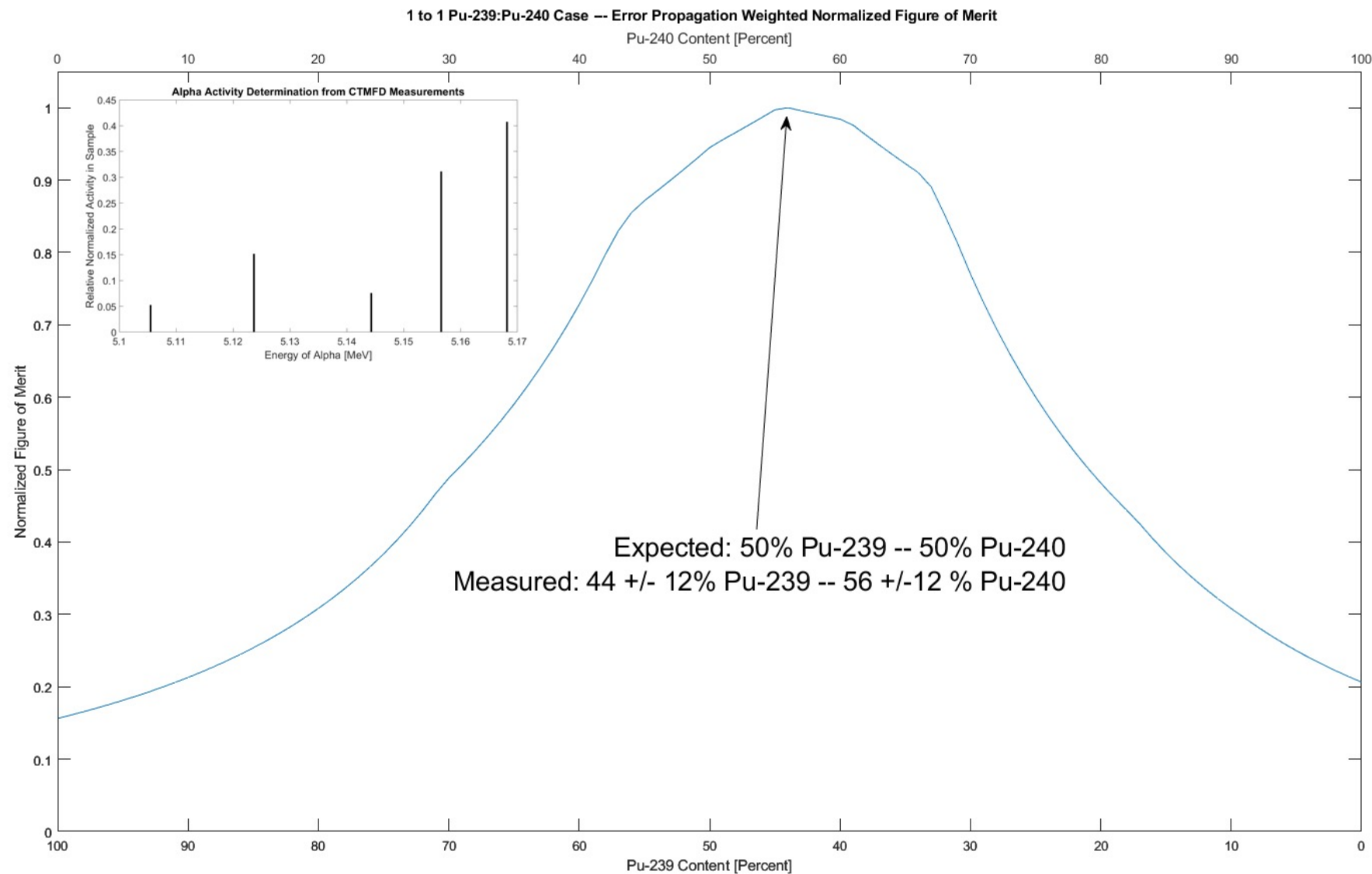


FIG. 13 Variation of FOM for 1:1 Activity Ratio (50% Pu-239; 50% Pu-240) & Predicted Alpha Energy Spectrum

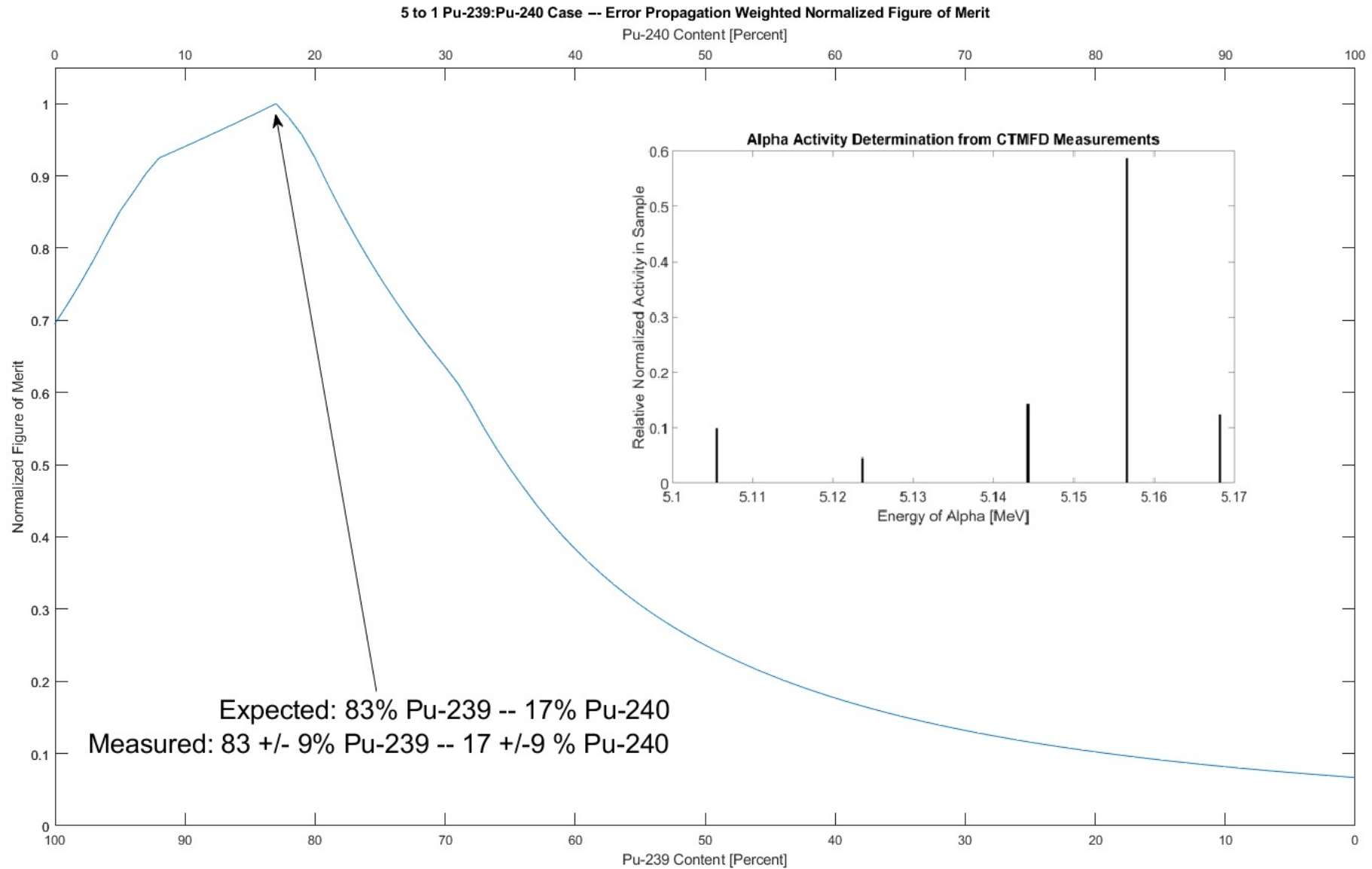


FIG. 14 Variation of FOM for 5:1 Activity Ratio (83% Pu-239; 17% Pu-240) & Predicted Alpha Energy Spectrum